



# Rules of fracture propagation of hydraulic fracturing in radial well based on XFEM

Xiaolong Li<sup>1</sup> · Wen Xiao<sup>2</sup> · Zhanqing Qu<sup>1</sup> · Tiankui Guo<sup>1</sup> · Jianxiong Li<sup>3</sup> · Wei Zhang<sup>1</sup> · Yu Tian<sup>1</sup>

Received: 27 August 2017 / Accepted: 14 January 2018 / Published online: 22 February 2018  
© The Author(s) 2018. This article is an open access publication

## Abstract

The radial well fracturing has been applied and achieved effective output. However, the fracture morphology and propagation law of it are still remain unclear, which limits the development and application of it. A 3D numerical model is established by ABAQUS to solve the current problems. The stage of fracture propagation is simulated by the extended finite element method. The conclusions stated that in situ stress field distribution was changed during the radial well fracturing and the induced stress field along the radial well is established at the same time. The propagation of major fracture is orientated by the induced stress in a certain area. The guiding function of fracture orientated propagation is evaluated by included angle  $\eta$  between the axis of radial well and equivalent fracture. The smaller the value of  $\eta$  is, the better effect of fracture orientated propagation is. The increase of horizontal stress difference and decrease of vertical density of radial wells are unfavorable to decrease the value of  $\eta$ . The failure pressure grows up with the azimuth angle of radial well increasing. The increasing of elastic modulus of formation is not conducive to the effect of radial well fracturing. The increasing of Poisson's ratio of formation is conducive to the failure pressure and maximum fracture width, but not as helpful as to decrease the value of  $\eta$ . Larger diameter of radial well is better for fracture oriented propagation. Operation parameters of fracturing fluid viscosity and construction displacement have less effect on the value of  $\eta$ . Also, the degree of different parameters influence on value of  $\eta$ , failure pressure and maximum fracture width is ranked by the grey correlation method. The results can be referred to prediction of fracture propagation and design of radial well completion or fracturing.

**Keywords** Radial well · Hydraulic fracturing · Induced stress field · Orientated propagation · XFEM

## Introduction

Radial well drilling by hydraulic jetting, whose length is up to 100 m and diameter is 25–50 mm, has been widely applied and has achieved positive effects, (Ma et al. 2005). Since the cost of radial well is far lower than horizontal well, the technique combining radial well and hydraulic fracturing as an emerging stimulation treatment comes into being. The emerging technique has been applied in several oil fields in

China, and performed a much better stimulation result than conventional perforation fracturing (Liu 2012). Studies have shown that radial well is capable of guiding the direction of fractures, which means the fracture propagation path can be controlled by radial well (Gong et al. 2016). Obviously, the performance of oriented fracture is not only effective in increasing the discharge area but also in developing the remaining oil. At present, it has been found out that the fracture initiates from the borehole of radial well (Gong et al. 2016). However, the study on radial well fracturing is still at the preliminary stage, the fracture morphology and propagation law of radial well fracturing still remain unclear, especially lacking visual achievement, which limits the development and application of radial well fracturing. Therefore, the mechanism and rules of fracture orientated propagation need to be revealed, which made the prediction of fracture propagation path practical.

To solve these problems currently, a 3D non-linear finite element numerical model based on fluid–solid coupling is established by ABAQUS. ABAQUS that is an authoritative

✉ Tiankui Guo  
guotiankui@126.com

Xiaolong Li  
lixiaolong199041@foxmail.com

<sup>1</sup> Department of Petroleum Engineering, China University of Petroleum (East China), QingDao 266580, China

<sup>2</sup> Petroleum Engineering Technology Institute of Shengli Oilfield, Dongying 610065, China

<sup>3</sup> College of Architecture & Environment, Sichuan University, Chengdu 610065, China

software in the field of stress analysis. In the model, extend finite element method (XFEM) is used to simulate the initiation and propagation of fracture in radial well fracturing. A comparison between physical experiment and numerical simulation is arranged to assure the objectivity and applicability of the simulation results. Since the results of simulation in ABAQUS are visual, the fracture morphology and propagation path are obtained intuitively.

## Model establishment of radial well fracturing

ABAQUS is capable of handling complex problems in fracture propagation of rock, fluid–solid coupling and so on. The parameters' effect on fracture propagation, failure pressure and maximum fracture width were studied and simulated through XFEM, which made the propagation path of fracture visible.

### Fluid–solid coupling equation

The changing of effective stress in porous medium leads to the changing of permeability and porosity of formation, for example, the changes of rock strength or even deformation is caused by the varying of pore fluid pressure in formation during fracturing. Consequently, the coupling between stress field and seepage field should be taken into consideration.

Stress balance equation can be obtained from principle of virtual work (Zienkiewicz and Taylor 2005):

$$\int_V \sigma \delta \varepsilon dV = \int_S t \delta v dS + \int_V \hat{f} \delta v dV \quad (1)$$

where  $\delta v$  is virtual velocity, m/s;  $\delta \varepsilon$  is virtual strain rate,  $s^{-1}$ ;  $f$  is the body force per unit volume,  $N/m^3$ ;  $t$  is the surface force per unit area,  $N/m^2$ ;  $\sigma$  is the total stress of porous medium, Pa.

The continuity equation of fluid medium can be obtained from mass conservation theorem:

$$\int_V \delta v \frac{1}{J} \frac{d}{dt} (J \rho_w n_w) dV + \int_V \delta v \frac{\partial}{\partial x} (\rho_w n_w v_w) dV = 0 \quad (2)$$

where  $J$  is the change rate of formation pore volume;  $n_w$  is the ratio of liquid volume to total volume in stratum;  $\rho_w$  is the liquid density in formation,  $kg/m^3$ ;  $X$  is the direction vector of fluid flow in the formation,  $m$ ;  $v_w$  is the flow rate in the formation, m/s.

The state of pore medium is determined by equation set which consists of Eqs. (1) and (2). The simultaneous equations equation with boundary condition is established.

Using the interpolation function introduced from finite element discretization method (Qingxia and Jie 2006), the simultaneous equation with boundary condition can be converted into stress-seepage coupling matrix finally (Lian 2007). Then, the matrix is calculated by the Newton method in ABAQUS.

### Extended finite element method and damage criterion

The core of XFEM is introducing additional functions to improve the displacement distribution of cell (Li and Wang 2005). For example, progressive function and discontinuous function are introduced to characterize the fracture tip, which ensure the fracture shape meanwhile improving the computational accuracy of the grid.

Function of fracture continuous displacement field is obtained from the simultaneous equation system of two level set functions which characterize fracture tip and fracture surface, respectively (Sepehri 2015):

$$u_{XFEM} = \sum_{i \in I} N_i(x) u_i + \sum_{j \in J} N_j(x) [H(x)] a_j + \sum_{k \in K_1} N_k(x) \left[ \sum_{l=4}^4 b_k^{l1} F_l^1(x) \right] + \sum_{k \in K_2} N_k(x) \left[ \sum_{l=4}^4 b_k^{l2} F_l^2(x) \right] \quad (3)$$

where  $N(x)$  is a collection of all nodes in a grid;  $F(x)$  is the shape function of fracture tip;  $u_i$  is the standard degree of freedom;  $J$  is the node set of the cells fracture crossing;  $H(x)$  is the extended shape function;  $a_j$  is the freedom degree of fracture surface;  $b_k^{l1}$ ,  $b_k^{l2}$  are the freedom degree of type I and type II fracture tip, respectively.

Process of material damage is divided into two stages (initial stage and evolution stage) in the model. When the material damage reaches the initial damage criterion, the fracture propagates by the rules of evolution. In the first stage, maximum principal stress (MAXPS) criterion is adopted to judge the damage initiation of material. The MAXPS criterion supposes that when the maximum principal stress reaches or exceeds a critical value, the material damage occurs. The formula of MAXPS is given:

$$f = \left\{ \frac{\langle \sigma_{\max} \rangle}{\sigma_{\max}^0} \right\} = 1 \quad (4)$$

where  $\sigma_{\max}^0$  is the maximum permissible principle stress.  $\langle \rangle$  is Macaulay brackets which means the damage won't occur under the condition of compression stress.

In the second stage, maximum energy release rate (MERR) criterion is adopted to judge the damage evolution of material. BK law is used for calculating the MERR in ABAQUS, and the formula is given (Chang et al. 2011):

$$G_{\text{equiv}C} = G_{IC} + (G_{IIC} - G_{IC}) \left( \frac{G_{III} + G_{II}}{G_{III} + G_{II} + G_I} \right)^n \quad (5)$$

where  $G_{\text{equiv}C}$  is critical fracture energy release rate, N/mm. It supposes that when the energy release rate of fracture tip exceeds the critical value, the tip split and the fracture propagation occurs.

$G_{IC}$ ,  $G_{IIC}$  are the normal and first tangential fracture toughness, respectively, N/mm;  $G_I$ ,  $G_{II}$ ,  $G_{III}$  are the normal, first tangential and second tangential fracture energy release rate, N/mm;  $n$  is the work of stress in the corresponding displacement.

At this point, a finite element model including in situ stress, rock mechanical properties and other factors is established in ABAQUS based on fluid–solid coupling. Also, the fracture initiation judged by MAXPS criterion and fracture propagation judged by MERR criterion are confirmed. The study of the rules of fracture propagation in radial well fracturing is done objectively and intuitively with the model.

### Model verification

The results of numerical model should be verified by the physical model experiment to prove the correctness of the numerical model. A 3D physical experiment in the laboratory is adopted to verify the numerical model whose experimental equipment is capable of simulating radial well fracturing with actual stress distribution both in horizontal and vertical direction. The test piece whose size is 0.3 m × 0.3 m × 0.3 m consists of cement and sand mixing in a proper proportion. Simulated wellbore with simulated radial well is placed in the center of the test piece. Water with red tracer is adopted as fracturing fluid. Experimental methods and procedures are same as literature (Jiang et al. 2014). The parameters of numerical simulation and physical experiment are shown in Table 1. The direction of maximum horizontal principal stress is defined as zero degree azimuth angle, so the azimuth of radial well is also the included angle between radial well and direction of maximum horizontal principal stress.

The fracture propagates along the radial well completely and the fracture surface is flat under the condition of 4 MPa horizontal stress difference. When the stress difference

increases to 6 MPa, the twists and turns occur during the fracture propagating. As is seen in Fig. 1, the simulation results match the results of experiment. Because the simulation result match the results of experiment, the correctness of the model is verified. The 3D extended finite element model based on fluid–solid coupling in ABAQUS is qualified to simulate radial well fracturing.

### Simulation and calculation

Data including information of reservoir, radial well and fracturing operation from a block in Shengli Oil Field, China are adopted as the parameters of the numerical model, which is shown in Table 2.

The property of formation material in the model is isotropic and homogeneous. Two radial wells are drilled central symmetrically and the fracture propagation rules of each radial well are supposed to be same, which means that the results of model present the fracture propagation rules of hydraulic fracturing in a single radial well. To improve the accuracy of calculation, the grids near the radial well and wellbore are refined, as seen in Fig. 2. Same as the definition in the previous chapter, X-direction is the direction of maximum horizontal principal stress and the positive half is defined as the 0° azimuth. Azimuth of radial well measured counterclockwise from the positive half of the x-axis is also the included angle between radial well and direction of maximum horizontal principal stress. Z-direction is the direction of vertical stress. Stress unit in the model is KPa, and tensile stress is positive.

The fracture propagation path is irregular and tortuous under the simulation of XFEM. For convenience, the concept of “equivalent fracture” is introduced. As seen in Fig. 3, within the same range of circular boundaries,  $S$  stands for the area that is enclosed by radial well and fracture, meanwhile  $S_{\text{eq}}$  stands for the area that enclosed by radial well and a given straight line connected to wellbore. When the value of  $S_{\text{eq}}$  is equal to the value of  $S$ , the given straight line is defined as the equivalent fracture of the corresponding real fracture; also the included angle between equivalent fracture and radial well is defined as equivalent deflection angle  $\eta$ . The value of  $\eta$  is adopted to evaluate the effect of radial well on fracturing propagation. Obviously, the smaller the

**Table 1** Table of experiment parameters

Elastic modulus (GPa)	Poisson's ratio	Maximum horizontal principal stress (MPa)	Minimum horizontal principal stress (MPa)	Permeability ( $\mu\text{m}^2$ )	Porosity (%)	Displacement in experiment (ml/min)	Azimuth of radial well ( $^\circ$ )
16.14	0.18	15	11 9	$15 \times 10^{-3}$	12	100	30

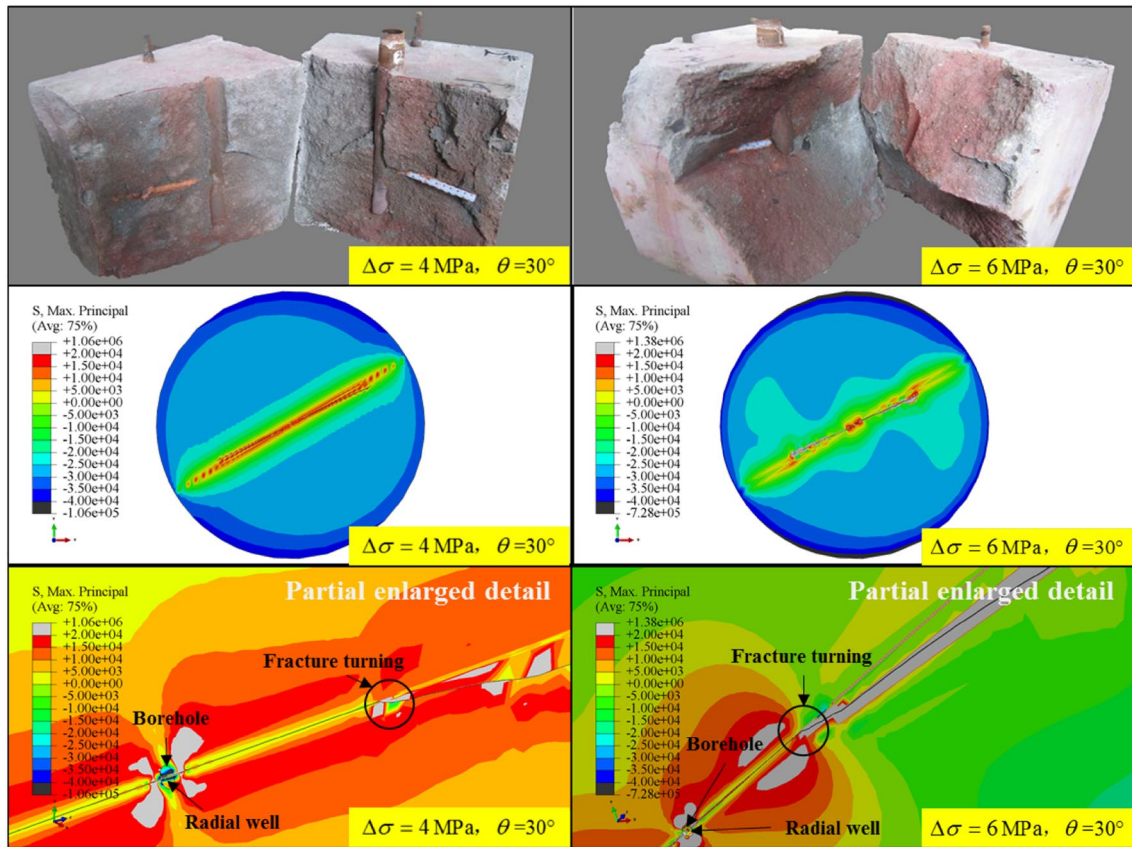


Fig. 1 Comparison of simulation results and experiment results

Table 2 Table of model parameters

Internal diameter of wellbore (mm)	240	Elastic modulus of formation (GPa)	20				
Diameter of formation (m)	150	Poisson's ratio of formation	0.22				
Thickness of formation (m)	0.2	Pore pressure (MPa)	15				
Diameter of radial well (mm)	50	Vertical stress (MPa)	35				
Length of radial well (m)	75	Maximum horizontal principal stress (MPa)	32.45	33.33	34.18	34.99	
Porosity (%)	25	Minimum horizontal principal stress (MPa)	26.43	25.33	24.18	22.99	
Tensile strength of rock (MPa)	3	Horizontal stress difference (MPa)	6	8	10	12	

value of  $\eta$  is, the better effect of radial well on fracturing propagation is.

## Calculation results and analysis

Different types of fracturing technique lead to different fracture morphologies (Zhang et al. 2008); the comparison of them is shown in Fig. 4. Under the condition of 6 MPa horizontal stress difference, 45° azimuth perforation, the  $\eta$  value of conventional perforation fracturing, orientated perforation fracturing and radial well fracturing are 45°, 30° and 4°, respectively. Obviously, the effect of radial well on guiding

the fracture propagation is confirmed and is much better than perforation fracturing (Jiang et al. 2009; Wang et al. 2005).

## Mechanism analysis of fracture orientated propagation

The parameters of azimuth of 45 and horizontal stress difference of 6 MPa are chosen as the benchmark, the mechanism of fracture orientated propagation in radial well fracturing is analyzed.

During fracturing, an induced stress field distributing along the radial well is formed because of the seepage of fracturing fluid from the perforation tunnel of radial well

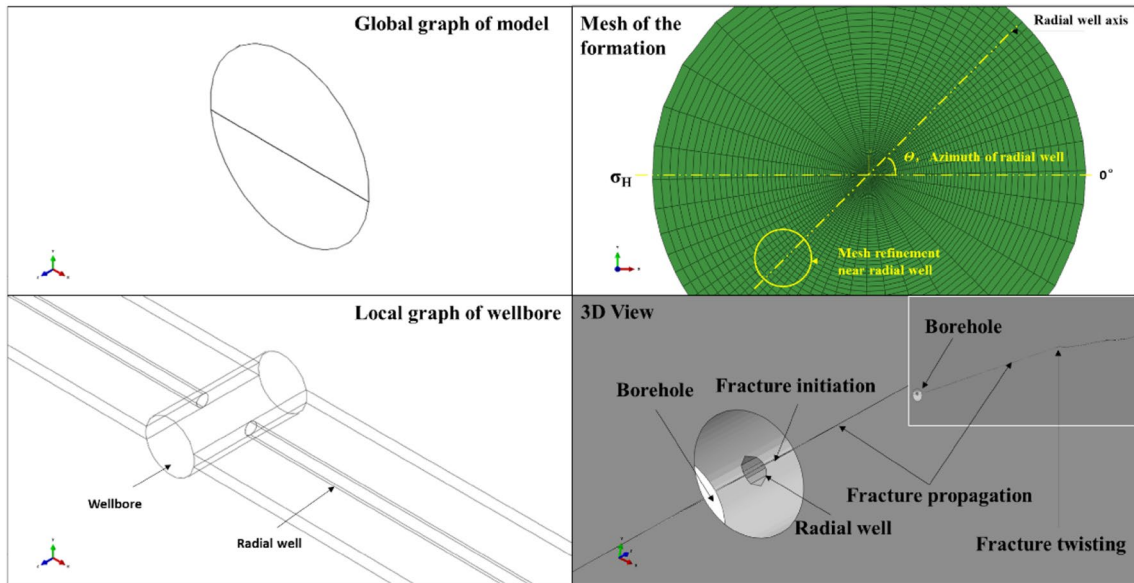


Fig. 2 Sketch of model

Fig. 3 Sketch of equivalent fracture

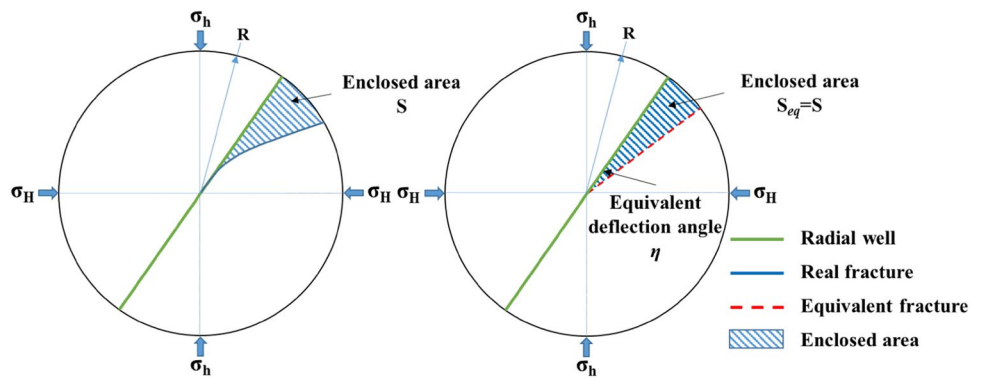
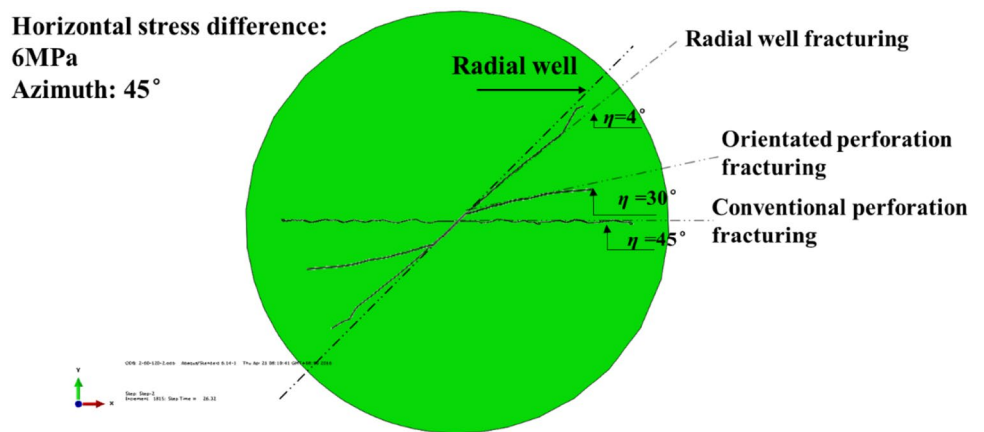


Fig. 4 Simulation results of different fracture types



to the formation. The magnitude and direction of in situ stress are changed by the induced stress field. As is seen in Fig. 5, the tensile stress which is formed in the induced stress field and perpendicular to the axis of the radial well

is the primary cause of fracture orientated propagation in radial well fracturing. Fracture turning to the direction of maximum horizontal principal stress is a trend caused by the horizontal stress difference of in situ stress. However,

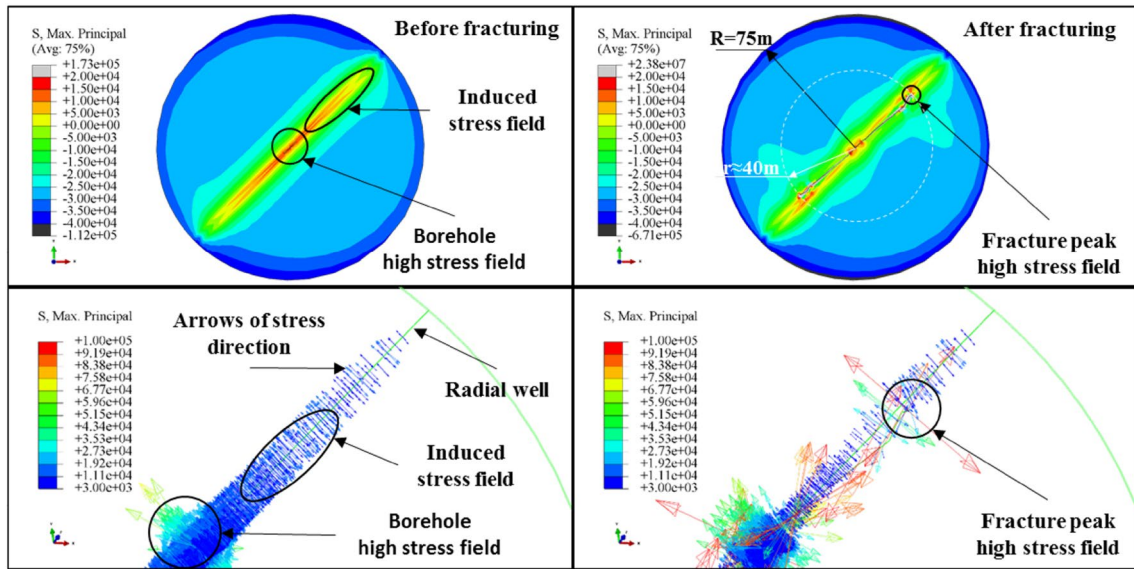


Fig. 5 Simulation results of induced stress field

since the in situ stress near the radial well is changed by the induced stress, the trend of fracture turning is weakened. Therefore, under the effect of both in situ stress and induced stress, the fracture propagates with a certain angle to the radial well. The induced stress field has effective range. In the range the fracture propagate along the radial well. When the fracture propagate out of the range, the in situ stress field is the only factor that influence the fracture propagation, the the fracture trend to turn to the direction of maximum horizontal stress. The effective guidance distance of radial well on fracture propagation is up to 40 m in this case.

“Max Principle” of the simulation results can be considered as “Maximum tensile stress” or “Minimum compressive stress”, since the tensile stress is positive in the model. According to the MAXPS criterion, when the value of Max

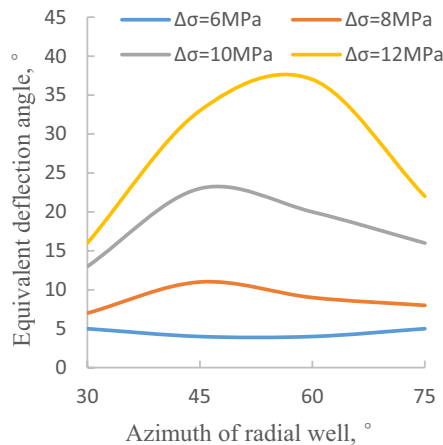
Principle is larger than the tensile strength of rock (3 MPa), the rock is supposed to crack. The range of visual results is adjusted to show the stress gradient in avoidance of the influence of high stress in the fracture tip.

### Influence of parameters on fracture propagation law

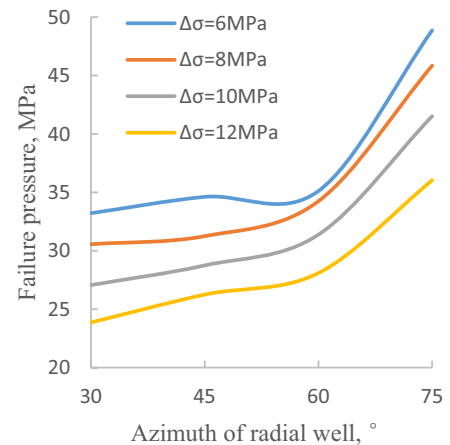
#### Radial well azimuth and horizontal stress difference

According to the simulation results (Fig. 6a), with the azimuth of radial well increasing, the value of  $\eta$  increases at first and then decreases, the maximum of  $\eta$  is at the azimuth of 45°. But, the influence rule of azimuth on  $\eta$  is not obvious.

Fig. 6 Influence law of azimuth angle on fracture propagation. **a** Chart of azimuth angle and angle  $\eta$  **b** Chart of azimuth angle and initiation pressure



(a) Chart of azimuth angle and angle  $\eta$



(b) Chart of azimuth angle and initiation pressure

Meanwhile the value of  $\eta$  increases obviously with increasing of horizontal stress difference, which means the condition of high horizontal stress difference is not conducive to the guidance function of radial well.

On the other hand, the failure pressure increases obviously with the increasing of azimuth and decreases with the increasing of horizontal stress difference (Fig. 6b), which means the condition of high horizontal stress difference is conducive to the initiation of fracture. The increasing amplitude of failure pressure is larger when the azimuth increases beyond 60°, which means high azimuth is not conducive to the initiation of fracture. The maximum fracture width and azimuth are not related. Also the maximum fracture width and horizontal stress difference are not related.

**Elastic modulus and Poisson’s ratio of formation**

Based on the model above, the parameters of azimuth of 45 and horizontal stress difference of 8 MPa are chosen as the

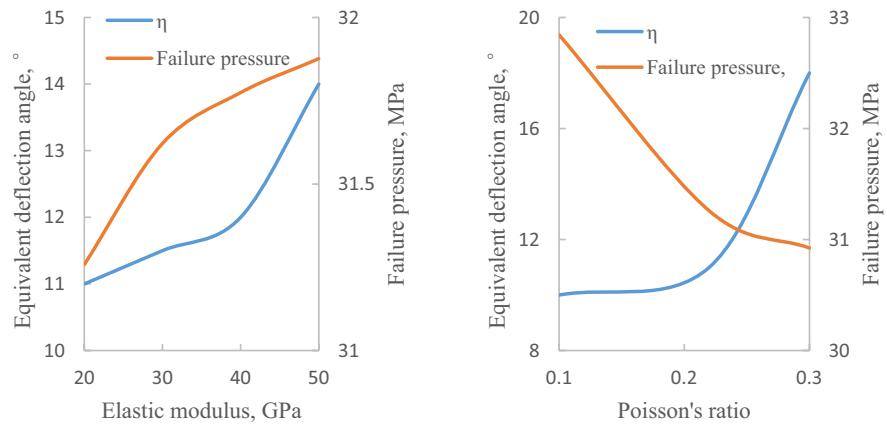
benchmark to analyze the influence of elastic modulus and Poisson’s ratio of formation on fracture propagation law.

According to the simulation results (Fig. 7), with the elastic modulus of formation increasing, the value of  $\eta$  and failure pressure increase slightly. Especially when the value of elastic modulus is smaller than 40 GPa, the influence of elastic modulus of formation on value of  $\eta$  is extremely little.

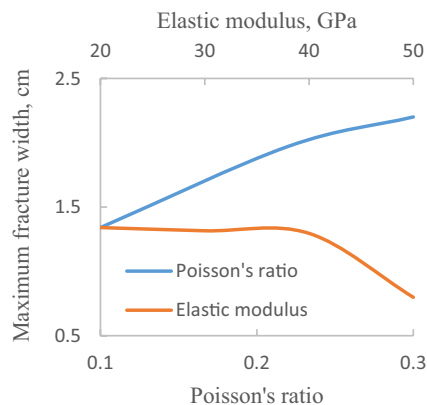
The value of  $\eta$  increases and the failure pressure decreases with the increasing of Poisson’s ratio of formation. When the value of Poisson’s ratio is larger than 40GPa, the influence of Poisson’s ratio of formation on value of  $\eta$  is greater.

The influence of elastic modulus and Poisson’s ratio of formation on maximum fracture width are much greater when compared to value of  $\eta$  or failure pressure. The increasing of elastic modulus is not conducive to the fracture initiation, orientated propagation and maximum fracture width. The increasing of Poisson’s ratio is conducive

**Fig. 7** Influence law of reservoir parameters on fracture propagation. **a** Chart of Young’s modulus and fracture propagation **b** chart of Poisson’s ratio and fracture propagation **c** chart of reservoir parameters and maximum crack width



**(a)** Chart of Young's modulus and fracture propagation **(b)** Chart of Poisson's ratio and fracture propagation



**(c)** Chart of reservoir parameters and maximum crack width

to the fracture initiation and maximum fracture width, but a little unfavorable to fracture orientated propagation

**Operation parameters**

Based on the model above, the parameters of azimuth of 45 and horizontal stress difference of 8 MPa are chosen as the benchmark to analyze the influence of fracturing fluid viscosity and construction displacement on fracture propagation law.

According to the simulation results (Fig. 8), with the increasing of fracturing fluid viscosity, the maximum fracture width and failure pressure increase slightly. Obviously, the influence of fracturing fluid viscosity on maximum fracture width is much greater. The value of  $\eta$  increases with the increasing of construction displacement but slightly.

The fracturing fluid viscosity and value  $\eta$  are not related. The displacement and maximum fracture width are not related.

**Vertical density of radial wells**

Based on the model above, the parameters of azimuth of 45 and horizontal stress difference of 6 MPa are chosen as the benchmark to analyze the influence of vertical density of radial wells on fracture propagation law.

According to the simulation results (Fig. 9), with the increasing of vertical density of radial wells, the value of  $\eta$  and failure pressure decrease obviously. When the vertical density of radial wells is less than 1 well per meter, the influence of radial well on fracturing propagation is weakened at a higher speed. So, the inflection point is 1 well per meter (Fig. 10).

The influence of vertical density of radial wells on maximum fracture width is not supposed to be laws neither according to the simulation results, so the curves of them are not shown.

**Diameter of radial well**

Based on the model above, the parameters of azimuth of 45 and horizontal stress difference of 8 MPa are chosen as the benchmark to analyze the influence of diameter of radial well on fracture propagation law.

**Fig. 8** Influence law of construction parameters on fracture propagation. **a** Chart of fracturing fluid viscosity and fracture propagation **b** chart of flow rate and fracture propagation

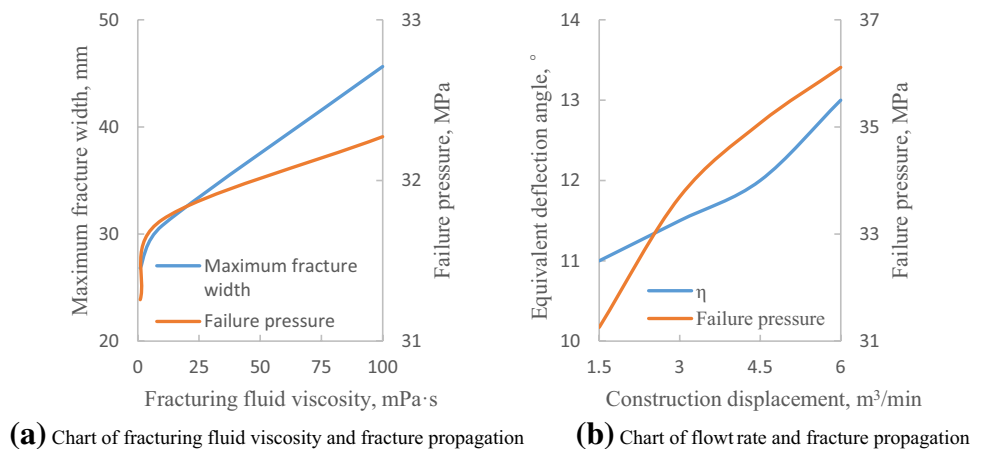


**Fig. 9** Influence law of reservoir thickness on fracture propagation

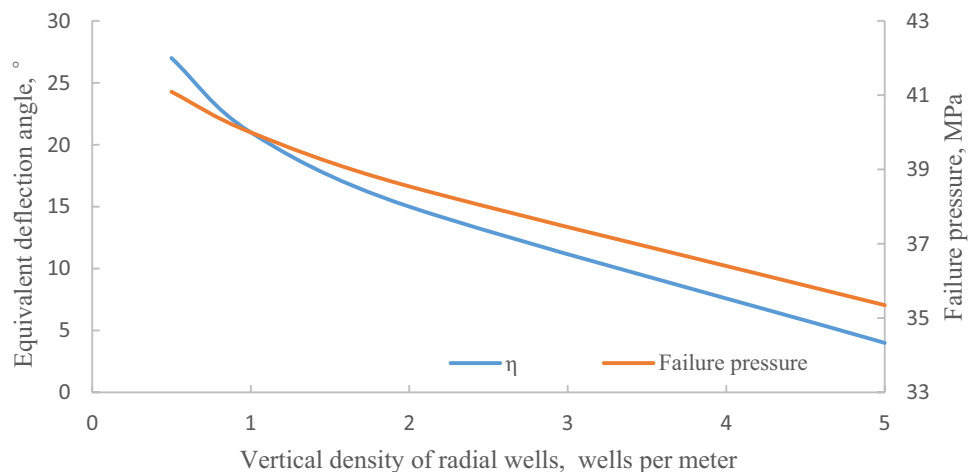
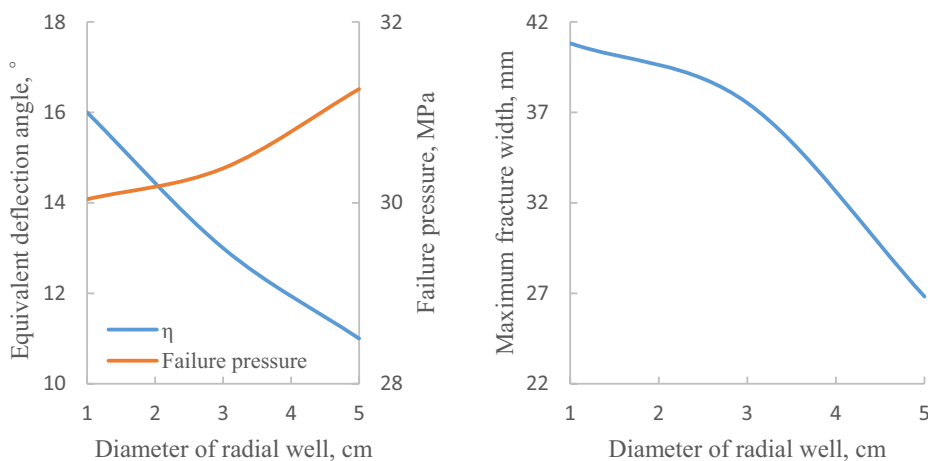




**Fig. 10** Influence law of reservoir thickness on fracture propagation. **a** Chart of diameter and fracture propagation **b** chart of diameter and maximum fracture width



**(a)** Chart of diameter and fracture propagation **(b)** Chart of diameter and maximum fracture width

According to the simulation results (Fig. 9), with the increasing of diameter of radial well, the value of  $\eta$  decreases obviously, meanwhile the failure pressure increases slightly. Apparently, large diameter of radial well is good for oriented propagation of fracturing. The maximum fracture width decreases with the increasing of diameter of radial well.

**Grey correlation analysis**

Grey correlation analysis uses a specific concept of information. It defines situations with no information as black, and those with perfect information as white. In fact, situations between these extremes are described as being grey. Therefore, a grey system means that a system in which part of information is known and part of information is unknown. With this definition, information quantity and quality form a continuum from a total lack of information to complete information from black through grey to white (Chan and Tong 2007).

Due to the limitation of simulation, grey correlation analysis is used as quantitative analysis of weight on the factors influencing fracture morphology. The detailed calculation steps and methods are shown in literature (Li et al. 2015). The brief steps of grey correlation analysis are shown below.

1. Confirm the reference sequence  $x_0(k)$  and comparison sequence  $x_i(k)$ .

2. Process non-dimensional treatment based on standardized method.
3. Calculate the correlation coefficient  $\xi_i(k)$ .

$$\xi_i(k) = \frac{\min_s \min_t |X_o(t) - X_s(t)| + \rho \max_s \max_t |X_o(t) - X_s(t)|}{|X_o(t) - X_s(t)| + \rho \max_s \max_t |X_o(t) - X_s(t)|} \quad (6)$$

where  $\rho$  is resolution coefficient and valued as 0.5 usually.

4. Calculate the correlation degree  $\gamma_i$ .

$$\gamma_i = \frac{1}{n} \sum_{k=1}^n \xi_i(k) \quad (7)$$

5. Sort the factors according to the correlation degree.

The reference sequence consists of azimuth, horizontal stress difference, elastic modulus of formation, Poisson’s ratio of formation, fracturing fluid viscosity, construction displacement, vertical density of radial wells and diameter of radial well. The comparison sequence consists of value of  $\eta$ , failure pressure and maximum fracture width. The correlation degree after calculating is shown in Table 3.

According to the calculation results, the top three largest components influencing the value of  $\eta$  is horizontal stress difference, vertical density of radial wells and

**Table 3** Data processing results

Factors	Azimuth	Horizontal stress difference	Elastic modulus	Poisson’s ratio	Viscosity	Construction displacement	Vertical density of radial wells	Diameter of radial well
Value of $\eta$	0.7910	<b>0.8761</b>	0.7876	0.7914	0.7078	0.7862	0.8244	0.7796
Failure pressure	<b>0.8291</b>	0.7947	0.7792	0.7817	0.7780	0.7673	0.8289	0.7875
Maximum fracture width	/	/	0.7664	0.7847	<b>0.7879</b>	/	/	0.7505

Bold values indicate the maximum value in results

Poisson's ratio of formation. The top three largest components influencing the failure pressure is azimuth, vertical density of radial wells and horizontal stress difference. The top three largest components influencing the maximum fracture width is fracturing fluid viscosity, Poisson's ratio of formation and elastic modulus of formation.

Since the horizontal stress difference is determined initially by formation and the azimuth is mostly determined by the distribution of remaining oil, the factor vertical density of radial well plays an important role in radial well fracturing. It can influence the fracture morphology both in propagation path and failure pressure greatly. Therefore, the factor vertical density of radial well is the key to the design of the radial well fracturing. The fracture width is mostly influenced by the rock properties.

## Conclusions

During fracturing, an induced stress field distributing along the radial well is formed because of the seepage of fracturing fluid from the perforation tunnel of radial well to the formation. The tensile stress which is formed in the induced stress field and perpendicular to the axis of the radial well is the primary cause of fracture orientated propagation in radial well fracturing. Therefore, under the effect of both in situ stress and induced stress, the fracture propagates with a certain angle to the radial well. The effective guidance distance of radial well on fracture propagation is up to tens of meters (40 m in this case). The effect of radial well on guiding the fracture propagation is much better than perforation fracturing.

The main factor influencing the fracture orientated propagation is horizontal stress difference. The increasing of horizontal stress difference is good for decreasing the failure pressure but not good for fracture orientated propagation. The azimuth of radial well influences the failure pressure mainly, which means low azimuth is good for fracture operation. The increase of vertical density of radial wells improves the effect of fracture orientated propagation greatly. The recommended vertical density of radial wells is larger or equal to 1 well per meter in this case. The increasing of elastic modulus of formation is not conducive to the fracture initiation, orientated propagation and maximum fracture width. The increasing of Poisson's ratio of formation is conducive to the fracture initiation and maximum fracture width, but not as helpful as to fracture orientated propagation. Large diameter of radial well is good for fracture orientated propagation. Operation parameters of fracturing fluid viscosity and construction displacement have less effect on fracture orientated

propagation and could be adjusted according to the actual situation.

As the parameters that can be controlled by human on the field, vertical density of radial well is the most crucial in the respect of guiding function of fracture orientated propagation. Therefore, the appropriate vertical density of radial wells is crucial. The azimuth is the most significantly influential factor on failure pressure, so the azimuth determines the operation difficulty. The selection of parameters needs to be considered and optimized according to the actual situation.

**Acknowledgements** The authors would like to acknowledge the financial support of the National Natural Science Foundation of China, China (Grant No. 51404288).

**Open Access** This article is distributed under the terms of the Creative Commons Attribution 4.0 International License (<http://creativecommons.org/licenses/by/4.0/>), which permits unrestricted use, distribution, and reproduction in any medium, provided you give appropriate credit to the original author(s) and the source, provide a link to the Creative Commons license, and indicate if changes were made.

## References

- Chan WK, Tong TKL (2007) Multi-criteria material selections and end-of-life product strategy, grey relational analysis approach. *Mater Des* 28(5):1539–1546
- Chang X, Chao H, Gang M, Zhao W (2011) Continuous-discontinuous deformable discrete element method to simulate the whole failure process of rock masses and application. *Chin J Rock Mech Eng* 30(10):2004–2011
- Gong DG, Qu ZQ, Guo TK, Tian Y, Tian KH (2016) Variation rules of fracture initiation pressure and fracture starting point of hydraulic fracture in radial well. *J Pet Sci Eng* 140:41–56
- Jiang H, Chen M, Zhang G et al (2009) Impact of oriented perforation on hydraulic fracture initiation and propagation. *Chinese J Rock Mech Eng* 28(7):1321–1326
- Jiang H, Shujie L, Baosheng H, Mian C, Guangqing Z (2014) Experiments of the oriented perforation impact on the multi-fracture pattern of hydraulic fracturing treatment. *J Nat Gas Ind* 34(2):66–70
- Li L, Wang T (2005) The extended finite element method and its applications—a review. *J Adv Mech* 35(1):5–20
- Li X, Wang B, Guo T, Gong F, Tian X, Huang Z (2015) Experiment on the friction test of the radial well based on gray correlation analysis. *J Pet Geol Oilfield Dev Daqing* 34(6):77–82
- Lian Z (2007) A simulation study of hydraulic fracturing propagation with a solid-fluid coupling model. D. University of Science and Technology of China
- Liu Y (2012) The research of increasing production mechanistic of radial direction drilling in low permeability reservoir. C. Northeast Petroleum University
- Ma K, Wu F, Yang Y, Fan Y, Yang H, Chen X (2005) Application of radial horizontal drilling technology in W5 well. *J Drill Prod Technol* 28(5):17–20
- Qingxia Y, Jie L (2006) A research on saturated soil dynamic response with ABAQUS. *J Earthq Eng Eng Vib* 26(3):238–241
- Sepehri J (2015) Pinnacle-A Halliburton Service. Application of extended finite element method (XFEM) to simulate hydraulic fracture from oriented perforations. Paper SPE presented at SPE Hydraulic Fracturing Technology held in woodlands, USA 3–15 February 2015

- Wang Z, Karamay X, Guo D, Deng J (2005) Effect of perforation mode on the fracturing pressure and cranny geometric shape. *J Southwest Pet Inst* 27(5):57–60
- Zhang GQ, Chen M (2009) Complex fracture shapes in hydraulic fracturing with orientated perforations1. *Petrol Explor Dev* 36(1):103–107

Zienkiewicz OC, Taylor RL (2005) *The finite element method, an introduction with partial differential equations*. M. Burlington, Elsevier, Amsterdam, pp 42–45

**Publisher's Note** Springer Nature remains neutral with regard to jurisdictional claims in published maps and institutional affiliations.